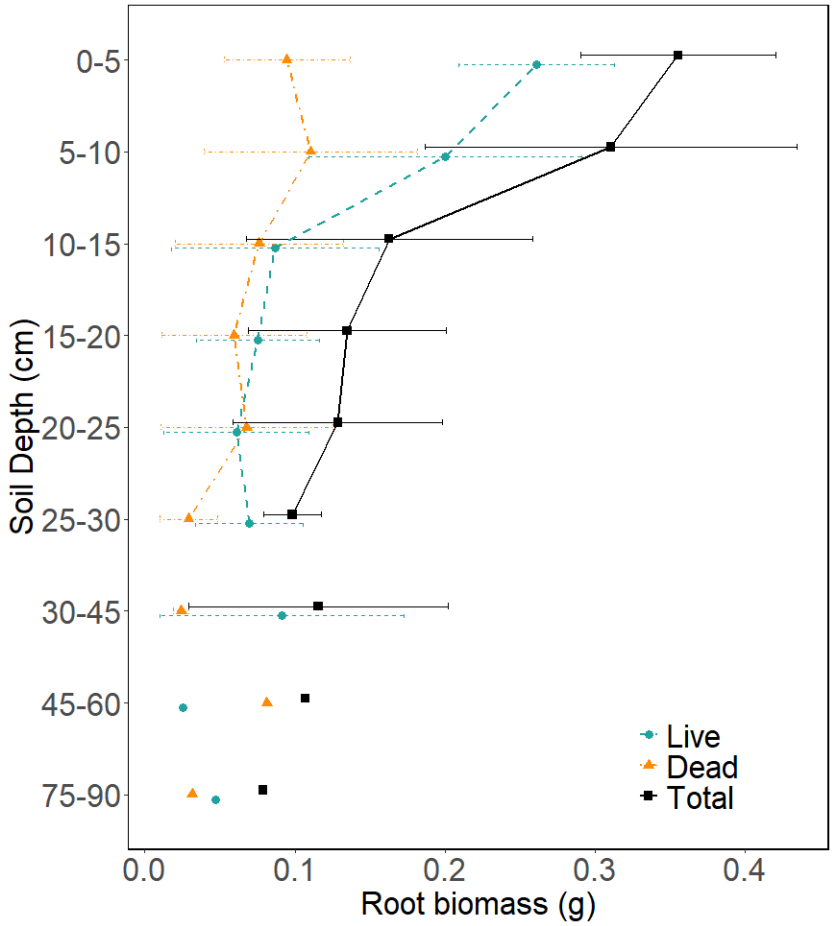

Figure. S1. Vertical profile of live, dead, and total fine root biomass at the AmeriFlux US-CRK site in February 2023. Error bars represent standard deviation among plots (n = 4).

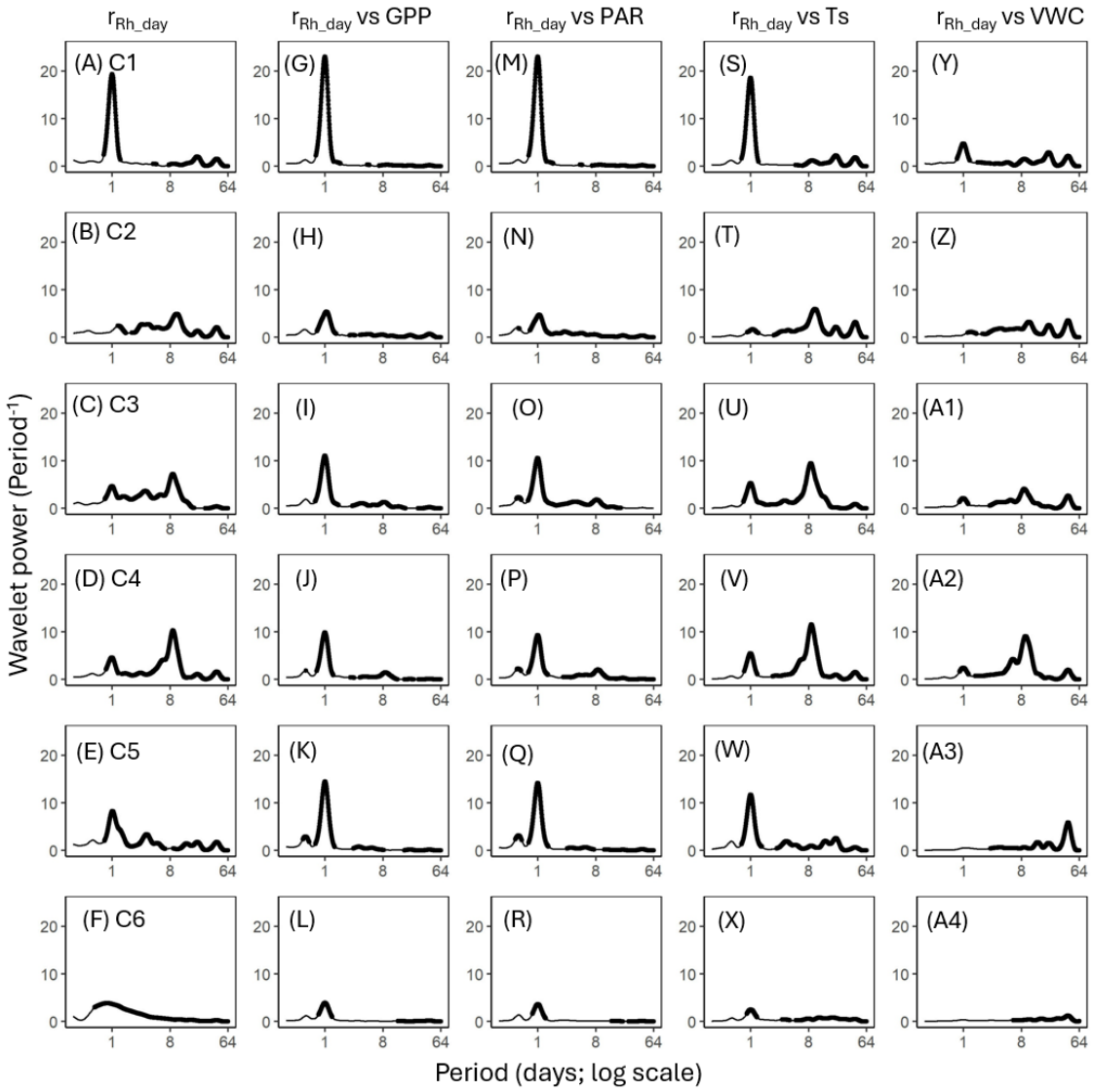

Figure S2. Average wavelet power in the frequency domain generated from the wavelet transformation of the model residual of heterotrophic respiration with coefficients estimated by each day (r_{Rh_day}; A–F) for six campaigns (C1–C6) at US-CRK. Average wavelet power in the frequency domain generated from the cross-wavelet transformation of r_{Rh_day} against gross primary productivity (GPP; G–L), photosynthetically active radiation (PAR; M–R), soil temperature (Ts; S–X), and volumetric water content (VWC; Y–A4) at 5-cm depth for six campaigns at the US-CRK site. The bold contours indicate areas with significant coherence at the 5% level against white noise.

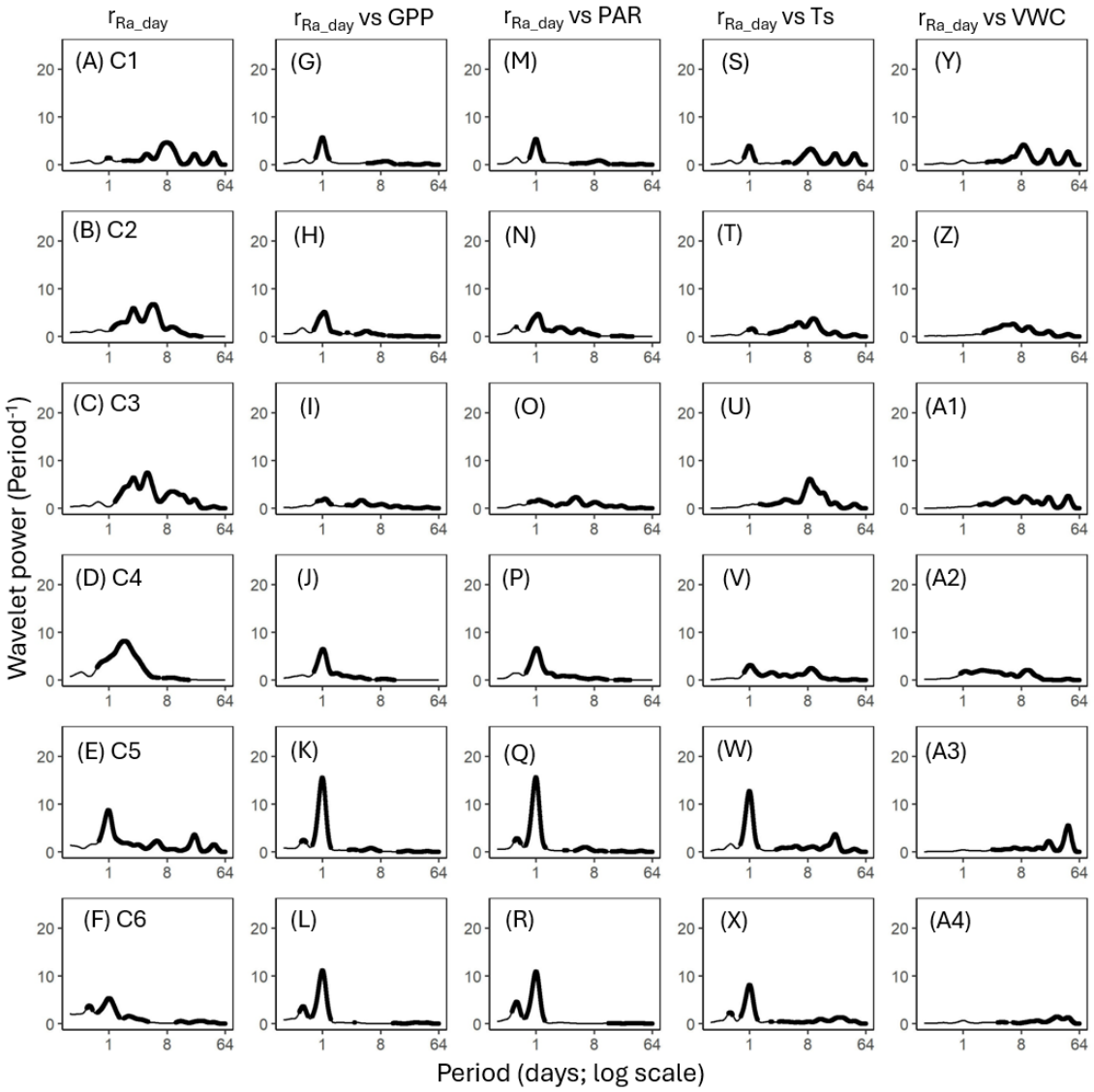

Figure S3. Average wavelet power in the frequency domain generated from the wavelet transformation of the model residual of autotrophic respiration with coefficients estimated by each day (r_{Ra_day}; A–F) for six campaigns (C1–C6) at US-CRK. Average wavelet power in the frequency domain generated from the cross-wavelet transformation of r_{Ra_day} against gross primary productivity (GPP; G–L), photosynthetically active radiation (PAR; M–R), soil temperature (Ts; S–X), and volumetric water content (VWC; Y–A4) at 5-cm depth for six campaigns at the US-CRK site. The bold contours indicate areas with significant coherence at the 5% level against white noise.

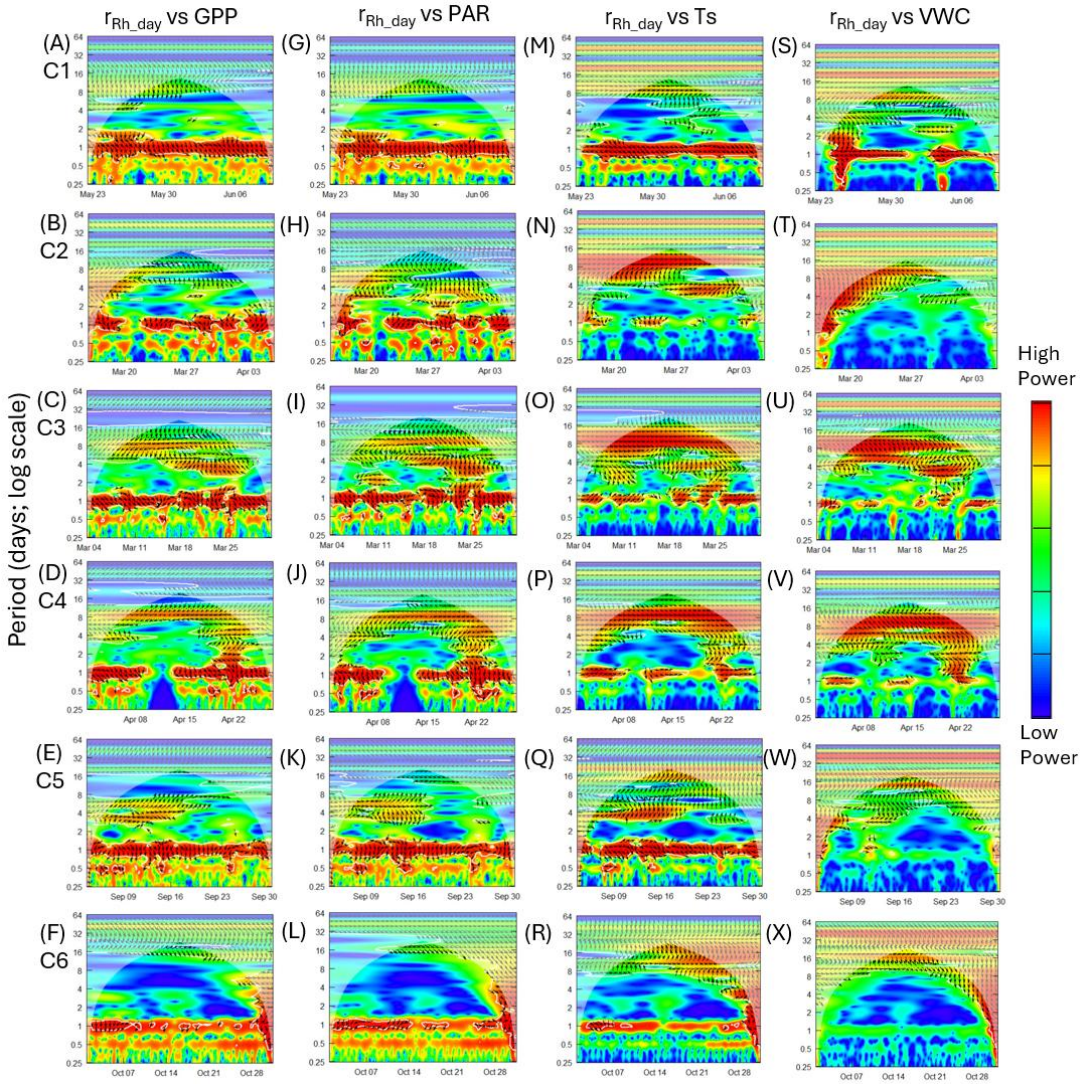

Figure S4: Heatmaps of the cross-wavelet transformation (XWT) of model residual of heterotrophic respiration with coefficients estimated by each day (r_{Rh_day}) against gross primary productivity (GPP; A–F), photosynthetically active radiation (PAR; G–L), soil temperature (Ts; M–R), and volumetric water content (VWC; S–X) for six measurement campaigns (C1–C6) at US-CRK. Arrows pointing to the right and left represent positive and negative correlations, respectively, without lag. Arrows pointing up-left (positive correlation) and down-right (negative correlation) indicate the response component lags behind the driver, while arrows pointing up-right and down-left indicate that the driver lags behind the response component. The 5% significance level of the XWT analysis was generated within the cone of influence (COI) against white noise and identified by white contour lines. COI within the heat plot is identified with a light shade.

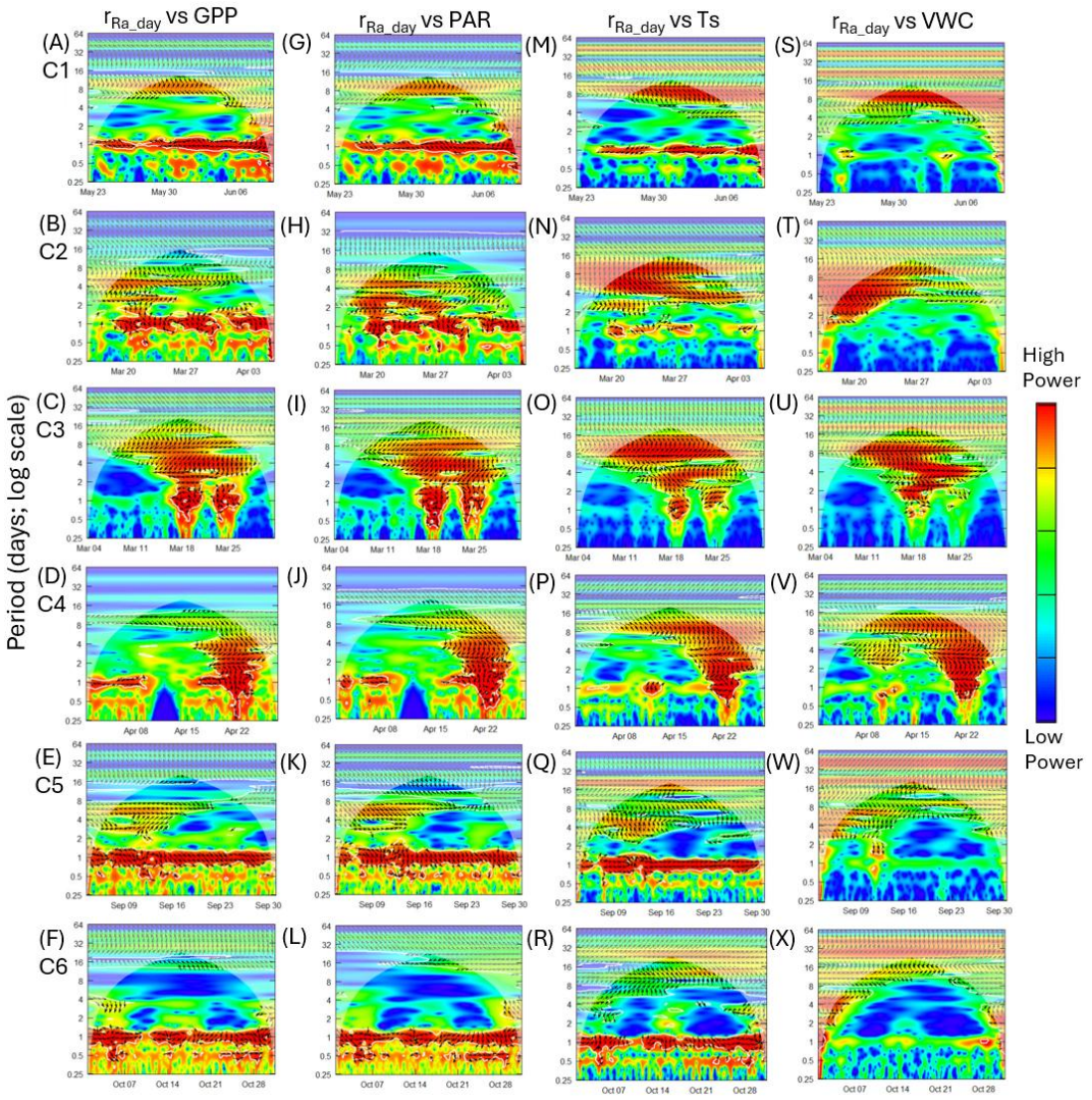

Figure S5. Heatmaps of the cross-wavelet transformation (XWT) of model residual of autotrophic respiration with coefficients estimated by each day (r_{Ra_day}) against gross primary productivity (GPP; A–F), photosynthetically active radiation (PAR; G–L), soil temperature (Ts; M–R), and volumetric water content (VWC; S–X) for six measurement campaigns (C1–C6) at US-CRK. Arrows pointing to the right and left represent positive and negative correlations, respectively, without lag. Arrows pointing up-left (positive correlation) and down-right (negative correlation) indicate the response component lags behind the driver, while arrows pointing up-right and down-left indicate that the driver lags behind the response component. The 5% significance level of the XWT analysis was generated within the cone of influence (COI) against white noise and identified by white contour lines. COI within the heat plot is identified with a light shade.

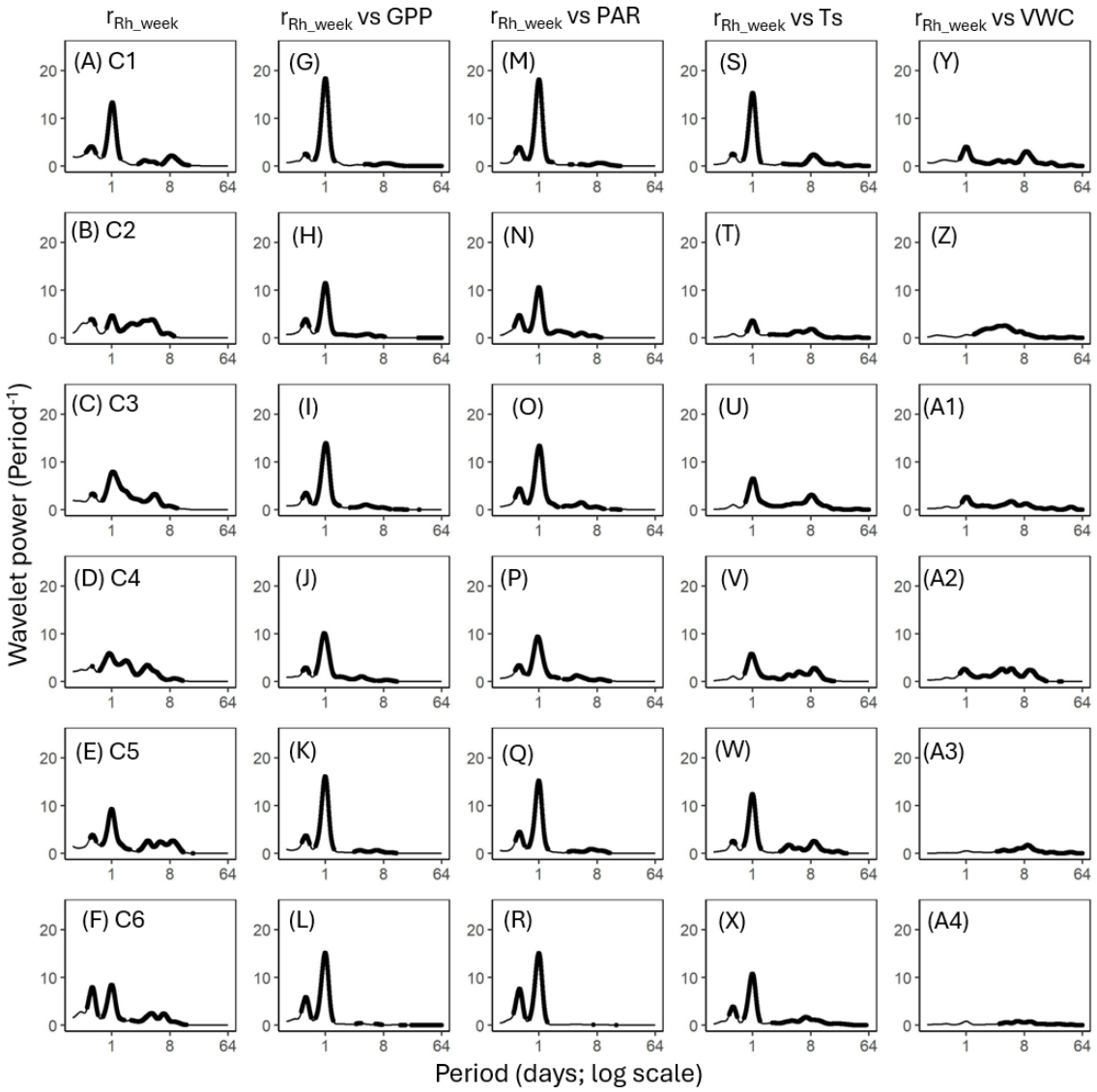

Figure S6. Average wavelet power in the frequency domain generated from the wavelet transformation of the model residual of heterotrophic respiration with coefficients estimated by weekly rolling windows (r_{Rh_week}; A–F) for six campaigns (C1–C6) at US-CRK. Average wavelet power in the frequency domain generated from the cross-wavelet transformation of r_{Rh_week} against gross primary productivity (GPP; G–L), photosynthetically active radiation (PAR; M–R), soil temperature (Ts; S–X), and volumetric water content (VWC; Y–A4) at 5-cm depth for six campaigns at the US-CRK site. The bold contours indicate areas with significant coherence at the 5% level against white noise.

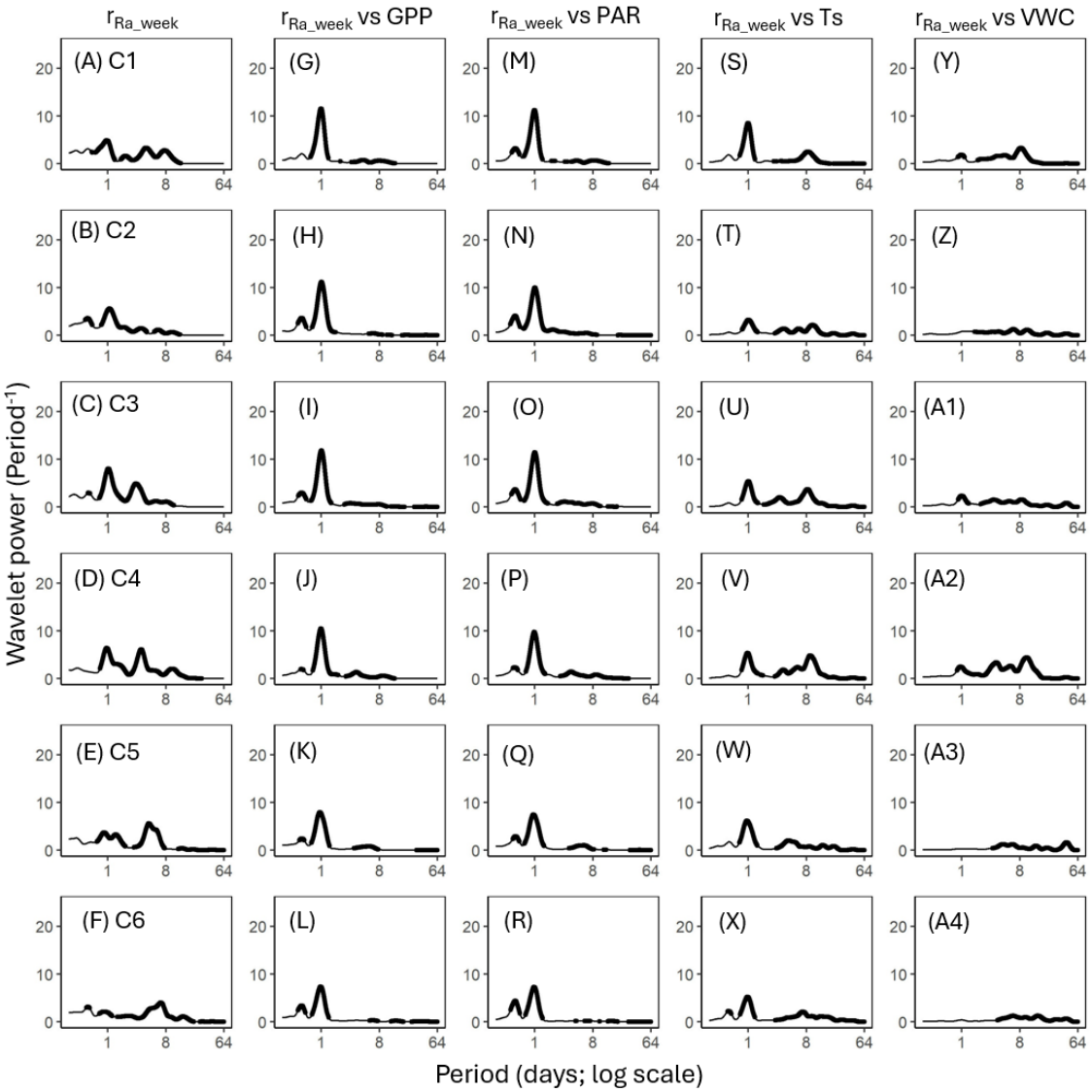

Figure S7. Average wavelet power in the frequency domain generated from the wavelet transformation of the model residual of autotrophic respiration with coefficients estimated by weekly rolling windows (r_{Ra_week}; A–F) for six campaigns (C1–C6) at US-CRK. Average wavelet power in the frequency domain generated from the cross-wavelet transformation of r_{Ra_week} against gross primary productivity (GPP; G–L), photosynthetically active radiation (PAR; M–R), soil temperature (Ts; S–X), and volumetric water content (VWC; Y–A4) at 5-cm depth for six campaigns at the US-CRK site. The bold contours indicate areas with significant coherence at the 5% level against white noise.

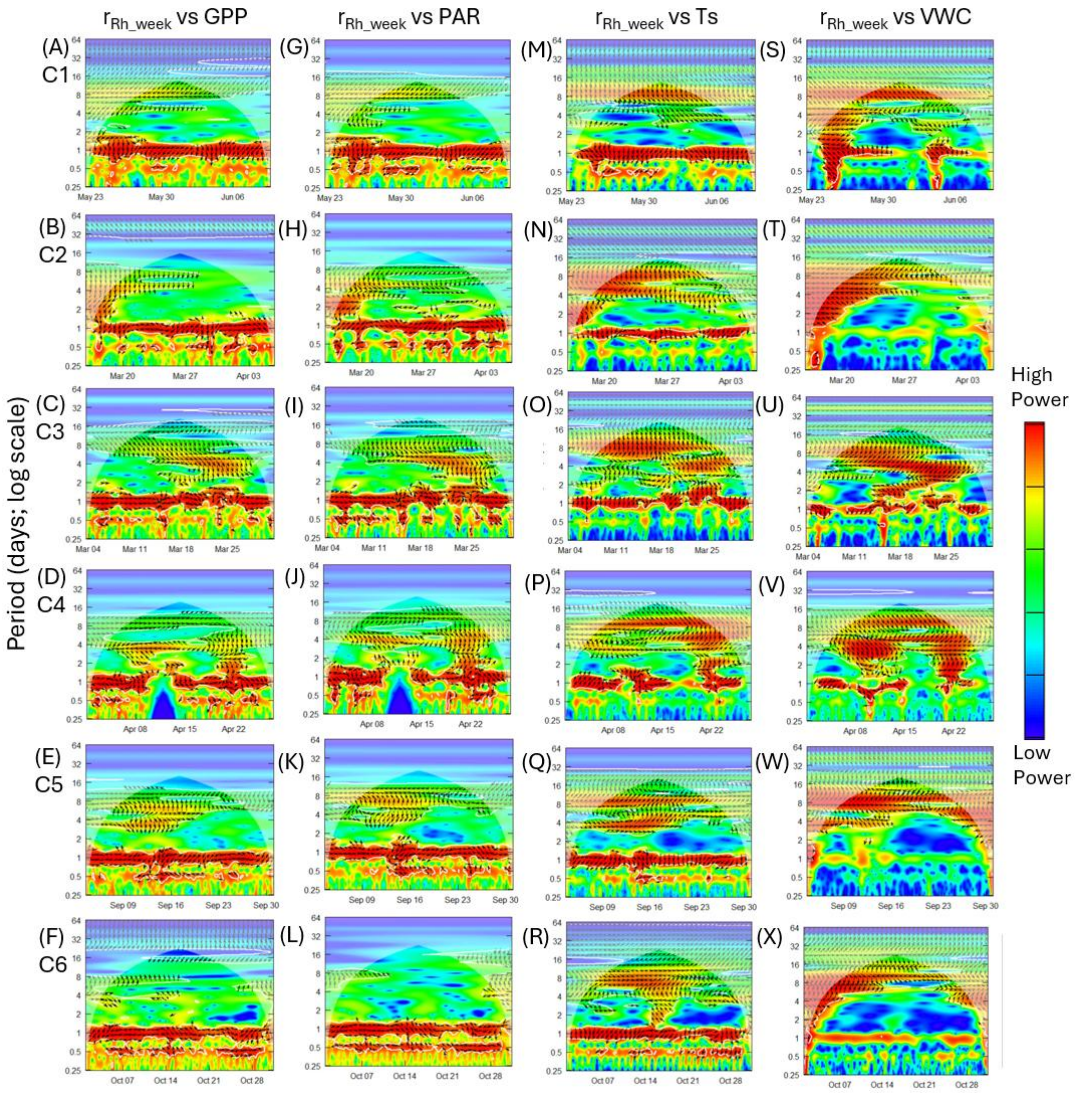

Figure S8. Heatmaps of the cross-wavelet transformation (XWT) of model residual of heterotrophic respiration with coefficients estimated by weekly rolling windows (r_{Rh_week}) against gross primary productivity (GPP; A–F), photosynthetically active radiation (PAR; G–L), soil temperature (Ts; M–R), and volumetric water content (VWC; S–X) for six measurement campaigns (C1–C6) at US-CRK. Arrows pointing to the right and left represent positive and negative correlations, respectively, without lag. Arrows pointing up-left (positive correlation) and down-right (negative correlation) indicate the response component lags behind the driver, while arrows pointing up-right and down-left indicate that the driver lags behind the response component. The 5% significance level of the XWT analysis was generated within the cone of influence (COI) against white noise and identified by white contour lines. COI within the heat plot is identified with a light shade.

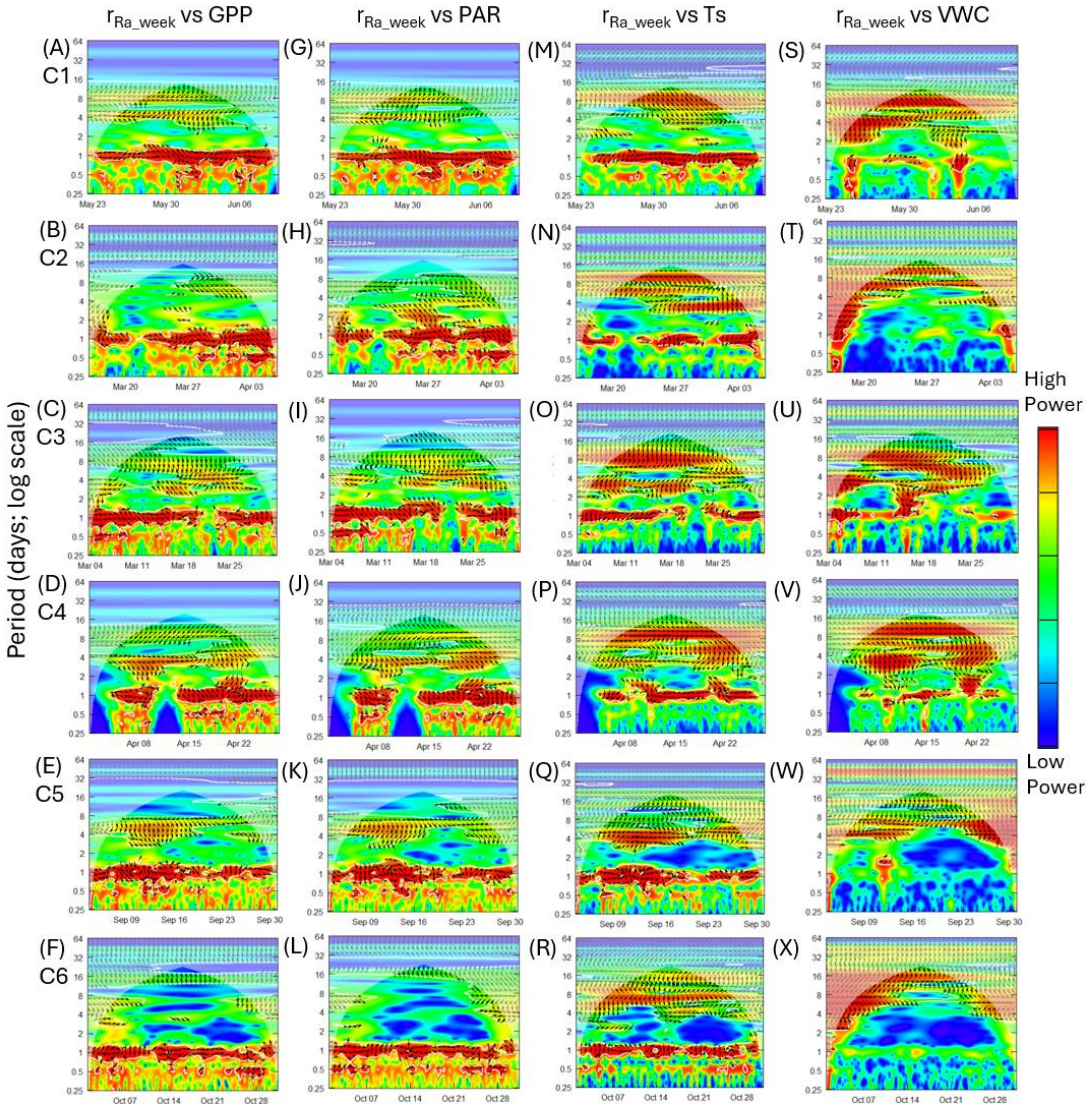

Figure S9. Heatmaps of the cross-wavelet transformation (XWT) of model residual of autotrophic respiration with coefficients estimated by weekly rolling windows (r_{Ra_week}) against gross primary productivity (GPP; A–F), photosynthetically active radiation (PAR; G–L), soil temperature (Ts; M–R), and volumetric water content (VWC; S–X) for six measurement campaigns (C1–C6) at US-CRK. Arrows pointing to the right and left represent positive and negative correlations, respectively, without lag. Arrows pointing up-left (positive correlation) and down-right (negative correlation) indicate the response component lags behind the driver, while arrows pointing up-right and down-left indicate that the driver lags behind the response component. The 5% significance level of the XWT analysis was generated within the cone of influence (COI) against white noise and identified by white contour lines. COI within the heat plot is identified with a light shade.

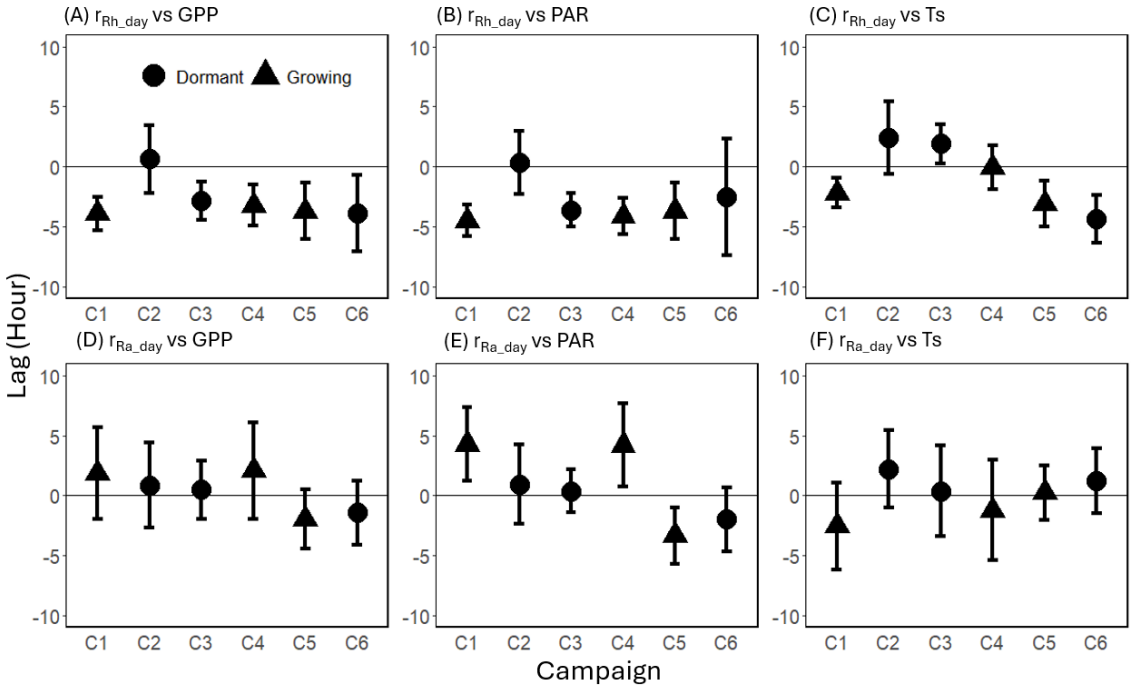

Figure S10. Mean time lag (± standard deviation) between model residual of heterotrophic respiration with coefficients by each day (r_{Rh_day}) and (A) gross primary productivity (GPP), (B) photosynthetically active radiation (PAR), and (C) soil temperature (Ts), and between model residual of autotrophic respiration with coefficients estimated by each day (r_{Ra_day}) and (D) GPP, (E) PAR, and (F) Ts at the diurnal frequency range (0.5 to 1.5 days) across six measurement campaigns (C1–C6). Phase differences were averaged over the diurnal frequency range and included only when the 1-day spectral peak was significant ($p < 0.1$). Round dots represent dormant season campaigns, while triangles represent growing season campaigns. Positive lag values indicate that respiration preceded the corresponding driver, while negative values indicate that respiration lagged behind the driver.

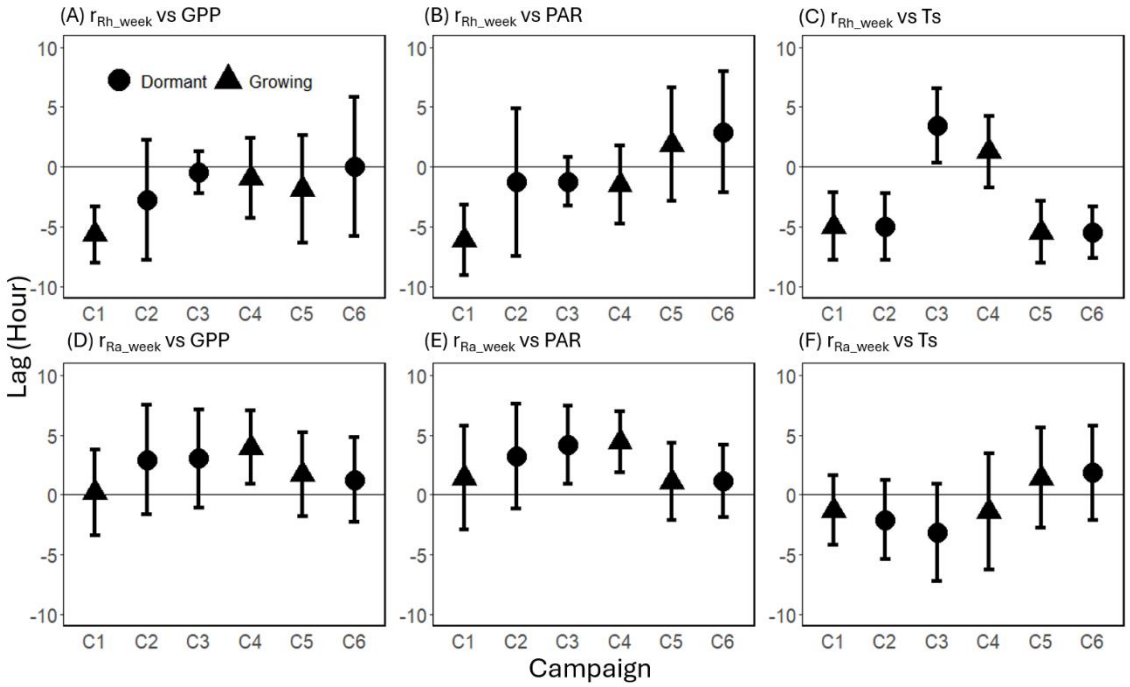

Figure S11. Mean lag times (± standard deviation, in hours) between model residual of heterotrophic respiration with coefficients estimated by weekly rolling windows (r_{Rh_week}) and (A) gross primary productivity (GPP), (B) photosynthetically active radiation (PAR), and (C) soil temperature (Ts), and between model residual of autotrophic respiration with coefficients estimated by weekly rolling windows (r_{Ra_week}) and (D) GPP, (E) PAR, and (F) Ts at the diurnal frequency range (0.5 to 1.5 days) across six measurement campaigns (C1–C6). Phase differences were averaged over the diurnal frequency range and included only when the 1-day spectral peak was significant ($p < 0.1$). Circular dots represent dormant season campaigns, while triangles represent growing season campaigns. Positive lag values indicate that respiration preceded the corresponding driver, while negative values indicate that respiration lagged behind the driver.

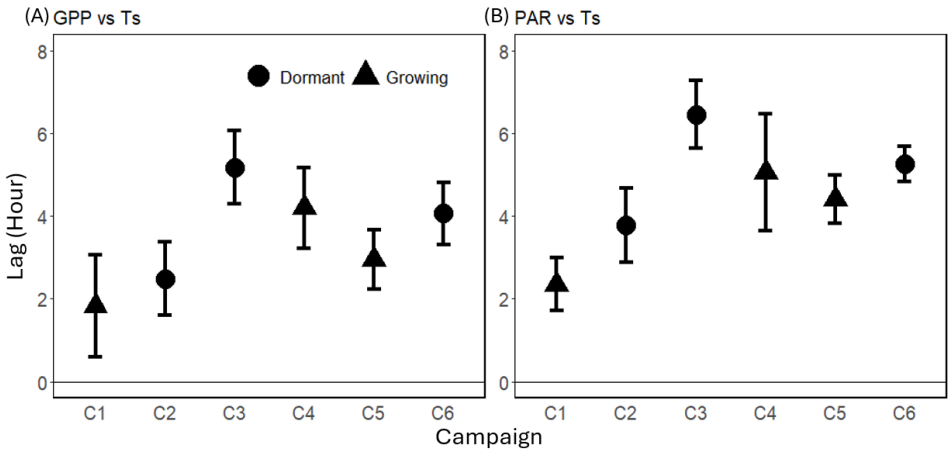

Figure S12. Mean lag times (± standard deviation, in hours) between (A) gross primary productivity (GPP) and soil temperature (Ts), and (B) photosynthetically active radiation (PAR), and Ts at the diurnal frequency range (0.5 to 1.5 days) across six measurement campaigns (C1–C6). Phase differences were averaged over the diurnal frequency range and included only when the 1-day spectral peak was significant ($p < 0.1$). Circular dots represent dormant season campaigns, while triangles represent growing season campaigns. Positive lag values indicate that respiration preceded the corresponding driver, while negative values indicate that respiration lagged behind the driver.